

Correlations in Polymer Melts and Solutions As Investigated by Fluorescence Nonradiative Energy Transfer: A Novel Comparison of Theory to Experiment by Fluorescence Intensity Decay Measurements

Alice S. Mendelsohn,[†] Monica Olvera de la Cruz,^{*,†,‡} and John M. Torkelson^{*,†,‡}

Departments of Materials Science and Engineering and of Chemical Engineering, Northwestern University, Evanston, Illinois 60208

Received December 29, 1992; Revised Manuscript Received July 29, 1993*

ABSTRACT: A theoretical analysis of donor fluorescence intensity decay for a system of donor and trap (acceptor) end-labeled polymers has been developed to account for the effects of Förster nonradiative energy transfer (NRET) as a function of experimentally important parameters in a monodisperse polymer melt: polymer molecular weight, ratio of trap to donor concentration, and fraction of unlabeled polymer in the mix. The model distinguishes between donor- and trap-labeled material and employs intermolecular correlation functions which have been calculated to describe the chain statistics of a given polymer system. The model has been extended to describe the effects of NRET in semidilute solutions of end-labeled polymer by accounting for the swelling of the polymer by solvent and incorporating different chain statistics in the analysis. The donor fluorescence decay profiles calculated for perfectly labeled polymers employing phenanthrene as donor and anthracene as trap exhibit dramatic changes as a function of polymer concentration in solution or polymer molecular weight in bulk polymer. Comparisons of experimental decay profiles for solutions of terminally phenanthrene- and anthracene-labeled polyisoprene in toluene (with imperfect labeling) were made to theoretical predictions for this specific system. The good quantitative agreement between theory and experiment even in this system of low chromophore content suggests that fluorescence techniques may prove important in the study of correlations and chain statistics in more complicated systems, including blends of bimodally distributed homopolymers as well as blends of unlike polymers.

Introduction

Fluorescence nonradiative energy transfer has been used in the study of solution and solid-state polymer systems¹⁻³¹ as it can be sensitive to both intramolecular and intermolecular interactions. A typical energy transfer experiment in a polymeric system involves labeling a system of polymer chains with two different chromophores, donors and acceptors (traps). The different labels may be on the same chain or different chains in varying positions, depending on the specific experiment. Absorption of light by a chromophore results in the promotion of an electron to an excited singlet state. This energy may be dissipated through internal conversion, through fluorescence, or nonradiatively via a mechanism known as Förster energy transfer. Nonradiative energy transfer (NRET) occurs through induction of a dipole oscillation in the (unexcited) acceptor or trap chromophore by the excited-state donor chromophore. The rate of energy transfer, $w(r)$, between the chromophores is a function of the distance r of separation between the donor and the trap. This rate was first derived by Förster, who described the decay of fluorescence intensity due to nonradiative energy transfer in the form of a diffusion equation.³² Because of the length-scale dependence of energy transfer, monitoring fluorescence intensity in a system of labeled polymers provides a measure of distances between labels on the molecular level of the polymer chain^{2,5,14-17} and therefore can act as a local probe of the macromolecular structure.

NRET studies on polymers have been applied to a variety of issues with largely qualitative results. Fluorescence spectroscopy has proven to be useful for char-

acterizing polymer compatibility in blends of polymers with similar glass transition temperatures,^{1,2} when differential scanning calorimetry provides little sensitivity, and has also been used to examine compatibility in block copolymer/homopolymer blends.^{3,4} The critical concentration for polymer coil overlap, c^* , that marks the transition between dilute and semidilute solution has been characterized through monitoring fluorescence and energy transfer as functions of solution concentration and polymer molecular weight for polystyrene solutions.^{5,6} Micellar structure in block copolymer blends⁷ and solutions,⁸⁻¹³ morphology of polymer colloids,¹⁴⁻¹⁶ and structure of membrane films¹⁷ and polymer blends, including interactions in blends affecting phase separation,^{18,28-30} have also proven to be areas where energy transfer techniques are applicable. More recently, fluorescence energy transfer has been expanded to examine diffusion processes in polymer melts,^{19,20} blends,²¹ and latex films,^{22,23} polymer self-diffusion in solution²⁴ and in the bulk,²⁵ and small-molecule diffusion in glassy polymers.²⁶ NRET has also shown sensitivity in measuring end-to-end distance distributions in flexible oligomers.²⁷ As fluorescence studies continue to contribute an increasing understanding of polymer systems, the capabilities of these techniques receive more theoretical scrutiny.

The many theoretical proposals as to potential uses for fluorescence techniques have generally been more quantitative in nature but do not always consider experimental constraints. Several studies have examined the use of fluorescence to measure the radius of gyration of a polymer chain.^{18,33} Blend structure,³⁴ coil sizes,³⁵ and chain stiffness³⁶ could potentially also be studied with these techniques. Fredrickson³⁷ has proposed that intramolecular and intermolecular correlations are verifiable through NRET. Examining a system of end-labeled polymers where one polymer chain is labeled with a donor chro-

[†] Department of Materials Science and Engineering.

[‡] Department of Chemical Engineering.

* Abstract published in *Advance ACS Abstracts*, November 1, 1993.

mophore and n chains ($n \gg 1$) are labeled with traps, Fredrickson³⁷ related the donor fluorescence intensity decay to intermolecular correlations. The basic approach to this problem involves modifying Förster's original expression³² for energy transfer in a purely random system of chromophores to take into account the correlations in a labeled polymer system.

However, to be handled from a practical standpoint, Fredrickson's³⁷ arguments must be expanded to consider a real experimental system with a certain finite ratio of donor-labeled chains to trap-labeled chains. In this study, we have constructed such a theoretical model in conjunction with experiments, allowing a comparison of theory to experiment on both qualitative and quantitative levels. While several NRET studies have recently been completed that combine theoretical analysis and experiments to provide highly quantitative details on the diffusion of small molecules^{21b,26} or polymers²² across polymer interfaces and on small chain end-to-end distances,²⁷ the present study is the first to combine theory and NRET experiments involving donor fluorescence intensity decay measurements to investigate quantitatively correlations in polymeric systems.

Background

A. Random System of Chromophores. Following Förster's original arguments,³² the decay of fluorescence intensity through migration of electronic excitation is expressed in the form of a diffusion equation (1). This expression describes donor-trap energy transfer as a function of the lifetime of the donor fluorescence in the absence of acceptors or traps, τ_0 , the positions of the traps relative to the donor, r , and the Förster radius, R_0^{DT} , the critical distance for energy transfer, where $H(t)$ is the normalized donor fluorescence intensity decay with time and n_T is the total number of traps.

$$-\frac{dH(t)}{dt} = \frac{H}{\tau_0} + \frac{H}{\tau_0} \sum_{k=1}^{n_T} \{R_0^{DT}/r_k\}^6 \quad (1)$$

This expression is integrated with respect to time to obtain

$$H(t) = e^{-t/\tau_0} \prod_{k=1}^{n_T} e^{-w(r_k)t} \quad (2)$$

where $w(r) = (1/\tau_0)(R_0^{DT}/r)^6$, the Förster rate of energy transfer. Since the positions r of the traps are unknown, $H(t)$ must be averaged over all possible trap positions using the probability distribution function $P(r) dr$:

$$\overline{H(t)} = e^{-t/\tau_0} \left[\int_0^{R_e} e^{-w(r)t} P(r) dr \right]^{n_T} \quad (3)$$

where R_e is the effective range of the donor-trap interaction, defined by Förster as $V = (4/3)\pi R_e^3$. If the traps are randomly distributed, $P(r) dr$ is equal to all possible positions $d^d r/V$, where d is the dimensionality, and the quantity is divided by V to maintain the dimensionless quality of the integral. In the limit of $R_e \rightarrow \infty$ and $n_T \rightarrow \infty$, this integral simplifies to

$$\overline{H(t)} = e^{-t/\tau_0} \exp\{\rho_T \int d^d r [e^{-w(r)t} - 1]\} \quad (4)$$

where ρ_T is the total number density of traps and is the result of the n_T/V term that arises in the expansion of the expression when n_T is large. Equation 4 can be solved in a straightforward manner, recovering Förster's result:

$$\overline{H(t)} = e^{-t/\tau_0} \exp\{-\sqrt{\pi}(R_0^{DT}/R_e)^3 n_T (t/\tau_0)^{1/2}\} \quad (5)$$

Haan and Zwanzig³⁸ describe diffusion-like Förster energy transfer between randomly distributed chromophores in a system with no trapping sites; energy

transfer can occur in either direction, from donor to "trap" or the reverse. The arguments leading to eq 5 only consider the donor-to-trap energy transfer. Equation 5 is the exact probability that one donor chromophore, initially excited at $t = 0$, has not transferred its energy to a nearby trap or returned to its ground state by time t . Subsequently, an approximate expression³⁷ was derived for the probability that, in a system of randomly distributed donor chromophores, the donor chromophore that is excited at $t = 0$ is still excited at time t :

$$\langle H(t) \rangle = e^{-t/\tau_0} \exp\left\{-\left[\pi C_T \frac{t}{\tau_0}\right]^{1/2}\right\} \quad (6)$$

where C_T is a dimensionless chromophore concentration, assuming an extremely dilute donor concentration such that donor-donor NRET may be neglected. However, this expression is sufficient only to describe energy transfer among randomly distributed chromophores. In a more general system, there will be correlations between the positions of donors and traps. In a system of chromophore-labeled polymers, correlations due to polymer connectivity and excluded-volume effects are also important. These correlations turn the task of finding the average decay intensity into a many-body problem, but the expression for the decay can be found in a relatively simple manner using few approximations.

B. Correlated System. To include correlations, the integral in eq 3 is rewritten, replacing the random distribution $P(r) dr$ with $g(r) d^3 r/V$, where $g(r)$ is the correlated distribution. Considering a $g(r)$ that is normalized such that $\int g(r) d^3 r/V = 1$ and defining $g(r)$ in terms of the correlation function $h(r)$, $\rho g(r) = \rho + \rho h(r)$, an expression for $\langle H(t) \rangle$ as a function of the correlation function can be obtained. This substitution yields

$$\begin{aligned} \langle H(t) \rangle &= e^{-t/\tau_0} \exp\left\{-\int d^3 r (\rho + \rho h(r))(1 - e^{-w(r)t})\right\} \\ &= e^{-t/\tau_0} \exp\left\{-\rho \int d^3 r (1 - e^{-w(r)t}) - \int d^3 r \rho h(r)(1 - e^{-w(r)t})\right\} \quad (7) \end{aligned}$$

The uncorrelated result, when $h(r) = 0$, is equivalent to eq 6; when correlations are included through $h(r)$, one recovers³⁷

$$\begin{aligned} \langle H(t) \rangle &= \\ &\exp\left\{-\frac{t}{\tau_0} - \left[\pi C \frac{t}{\tau_0}\right]^{1/2} - \rho \int d^3 r h(r)(1 - e^{-w(r)t})\right\} \quad (8) \end{aligned}$$

where $C = (4/3)\pi(R_0^{DT})^3 \rho$ and ρ = the total number density of the chromophores.

Thus, part of the challenge is to use the proper correlation function in the expression for donor fluorescence intensity decay, which can then be compared to experimental results. In Fredrickson's analysis,³⁷ de Gennes³⁹ correlation function for a melt of end-labeled deuterated chains was used, and no distinction was made between donors and traps during the development of the model. This is not critical for the case Fredrickson³⁷ considered: a system with one donor and n traps. However, energy transfer is not readily observable experimentally when the concentration of donors is extremely dilute. To examine donor fluorescence intensity decay in a system with finite donor concentration, however, the possibility of donor-donor NRET must also be considered. Therefore, it is necessary to account for donor-donor spatial correlations as well as donor-trap correlations.

In order to do this properly, the expression for $\langle H(t) \rangle$ (eq 8) must be modified. Following the results of Nieuwoudt and Mukamel,⁴⁰ who used a cluster expansion technique³⁸ and resummation to determine a self-consis-

tent equation for intensity decay with time, the donor fluorescence intensity is calculated to first order in donor and trap concentrations. Equation 7 is rewritten more accurately as

$$\langle H(t) \rangle = e^{-t/\tau_0} \exp\left\{-\int d^3r (\rho_T + \rho_D h_{DT}(r))(1 - e^{-w_{DT}(r)t})\right\} \exp\left\{-\frac{1}{2}\int d^3r (\rho_D + \rho_D h_{DD}(r))(1 - e^{-2w_{DD}(r)t})\right\} \quad (9)$$

ρ_T and ρ_D are the number densities of traps and donors, respectively; $h_{DT}(t)$ is the donor-trap correlation function and $h_{DD}(r)$ is that for donor-donor spatial correlations. (The second integral in eq 9 has a factor of 2 multiplying the Förster rate of NRET since donor-donor transfer is a reversible process. The integral is also divided by 2 to avoid double-counting donors.) This leads to a final expression for the donor fluorescence intensity decay that includes all relevant correlations and interactions:

$$\langle H(t) \rangle = \exp\left\{-\frac{t}{\tau_0} - \left[\pi C_T \frac{2t}{\tau_0}\right]^{1/2} - \left[\pi C_D \frac{2t}{2\tau_0}\right]^{1/2}\right\} \times \exp\left\{-\rho_T \int d^3r h_{DT}(r)(1 - e^{-w_{DT}(r)t})\right\} \times \exp\left\{-\frac{\rho_D}{2} \int d^3r h_{DD}(r)(1 - e^{-2w_{DD}(r)t})\right\} \quad (10)$$

where $C_T = (4/3)\pi(R_0^{DT})^3\rho_T$ and $C_D = (4/3)\pi(R_0^{DD})^3\rho_D$. The term containing C_D describes the uncorrelated result for donor-donor NRET and is equivalent to the first-order term in Fredrickson's³⁷ density expansion describing energy transfer among uncorrelated donors.

In our approach, we derive the necessary correlation functions for a more general end-labeled polymer system using an expression that distinguishes between donors and traps, allowing variation of the relative amounts and chain lengths of donor- and trap-labeled chains. In this manner, the donor-trap and donor-donor correlation functions can be calculated for a specific experimental system, and the theoretical results can be eventually compared to those obtained experimentally. We also calculate $\langle H(t) \rangle$ in a semidilute solution of donor- and trap-labeled chains using scaling concepts. The aim of this study is to test the scaling hypothesis in the asymptotic semidilute regime. We find that predicted behavior of $\langle H(t) \rangle$ is sensitive to the trap-to-donor ratio in a system and polymer molecular weight as well as solution concentration which can be directly related to the value of the blob size ξ above which the chains overlap.

Application

A. Analysis of the Correlation Function. The correlation function for the melt of end-labeled chains is calculated using the random-phase approximation (RPA)³⁹ developed by de Gennes for calculating the correlation function of a melt of end-labeled deuterated chains. The RPA calculation results in an expression for $h(k)$, the Fourier transform of $h(r)$. The correlation function $h(k)$ is equal to the mean-square density fluctuations in the system: $h(k) = \langle \rho_k^i \rho_{-k}^j \rangle$. The calculation of $h(k)$ involves constructing the probability, $P[\{\rho_k\}] \prod_k d\rho_k$, for the system including the relevant chain statistics. For a melt of polymer chains, a Gaussian distribution function is employed. The donor-trap correlation function for a monodisperse melt of donor- and trap-labeled chains is equal to the mean-square density fluctuations for traps and donors, σ_k^T and σ_{-k}^D . The expression can also be written in terms of Debye functions, $D(x)$, and "half-Debye functions", $D^{1/2}(x)$, where $D(x) = (2N^2/x^2)(x + e^{-x} - 1)$ and

$$D^{1/2}(x) = (N/x)(1 - e^{-x}):$$

$$h_{DT}(k) = \langle \sigma_k^T \sigma_{-k}^D \rangle = \frac{-\rho_T \rho_D D_T^{1/2} D_D^{1/2}}{\rho_T D_T + \rho_D D_D} \quad (11)$$

(see Appendix A) where ρ_T and ρ_D are the relative number densities of traps and donors, respectively, and $x = (kR_g)^2$, where R_g is the polymer radius of gyration and N is the number of repeat units in the polymer chain. If the molecular weights of the donor- and trap-labeled chains are equal, then $D(x) = D_T(x) = D_D(x)$ and $D^{1/2}(x) = D_T^{1/2}(x) = D_D^{1/2}(x)$; eq 11 then simplifies to

$$h_{DT}(k) = \langle \sigma_k^T \sigma_{-k}^D \rangle = \left(\frac{\rho_T \rho_D}{\rho_T + \rho_D} \right) \frac{(1 - e^{-x})^2}{2(1 - x - e^{-x})} \quad (12)$$

where the term containing exponential functions is equivalent to the expression for $h(k)$ derived by de Gennes. The first term containing ρ_T and ρ_D accounts for varying amounts of traps and donors in the system. Distinguishing between the donor- and trap-labeled chains and allowing for variation of molecular weight of the two types of chains also will enable the study of correlations in, for example, a bimodal blend. This will be discussed in a future paper.⁴¹

To find $h_{DT}(r)$, the Fourier transform of $h_{DT}(k)$ given in eq 12 is determined. To simplify the Fourier transform integral (eq 13), only the magnitude of k is considered and an approximation for the Debye function⁴² is used:

$$h_{DT}(r) = \frac{1}{(2\pi)^3} \int h_{DT}(k) e^{-ik \cdot r} d^3k \quad (13)$$

This approximation has been employed previously^{42,43} and is considered accurate within 15% over the entire range of k . Substituting eq 12 into eq 13 results in

$$h_{DT}(r) = \frac{1}{4\pi^2} \left(\frac{\rho_T \rho_D}{\rho_T + \rho_D} \right) \int_0^\Lambda \frac{(1 - e^{-x})^2}{2(1 - x - e^{-x})} \frac{k}{r} \sin(kr) dk \quad (14)$$

where $\Lambda = 2\pi/l$. The segment length l establishes a minimum size scale for the system,⁴³ so Λ is a natural limit for the integral with respect to k . When l is small, $\Lambda \rightarrow \infty$ and the integration using the approximation for the Debye function⁴² in eq 14 can be done analytically. (See Appendix B.) The donor-donor correlation function is determined in an identical manner. The donor-trap correlation function (eq 15) describes the deviation from a purely random system:

$$h_{DT}(r) = \frac{-1}{\pi^2 r} \left(\frac{\rho_T \rho_D}{\rho_T + \rho_D} \right) \left\{ \frac{\pi}{2R_g^2} \exp(-2^{1/2}r/R_g) \right\} \quad (15)$$

as $h_{DT}(r) = g_{DT}(r) - 1$, it follows that $h_{DT}(r)$ is negative. Figure 1 shows the "correlation hole", exhibiting the depletion of donor-trap contacts at short distances, due to screening by other polymer chains. It should be noted that as the ratio of traps to donors increases, the donor-trap correlation function approaches zero; donors and traps are becoming more uncorrelated on all length scales.

B. Label Efficiency Effect. The correction term $(\rho_T \rho_D / (\rho_T + \rho_D))$ to de Gennes' correlation function³⁹ has a clear effect on the depth and width of the correlation hole for a donor- and trap-end-labeled polymer melt. ρ_T and ρ_D are defined such that $\rho_T + \rho_D \sim 1/N$ for the case of perfect end labeling (one label per chain of N repeat units). Varying the ratio of traps to donors, ρ_T/ρ_D , where $\rho_T/\rho_D = A$, results in a change in the donor fluorescence intensity decay profile as seen in Figure 2 where eq 10 has been used to calculate $\langle H(t) \rangle$ for an end-labeled polyisoprene melt for varying A . A polymer molecular weight of 90 000 has been used, as have the energy transfer param-

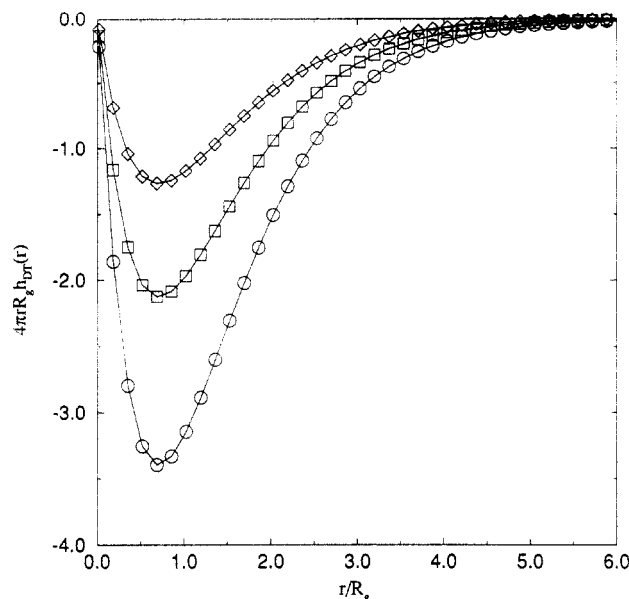


Figure 1. Correlation function calculated for a melt using the random-phase approximation, distinguishing between trap- and donor-end-labeled chains. $N = 1321$ (MW = 90 000), $\rho_T/\rho_D = A$: (O) $A = 2$, (\square) $A = 5$, (\diamond) $A = 10$.

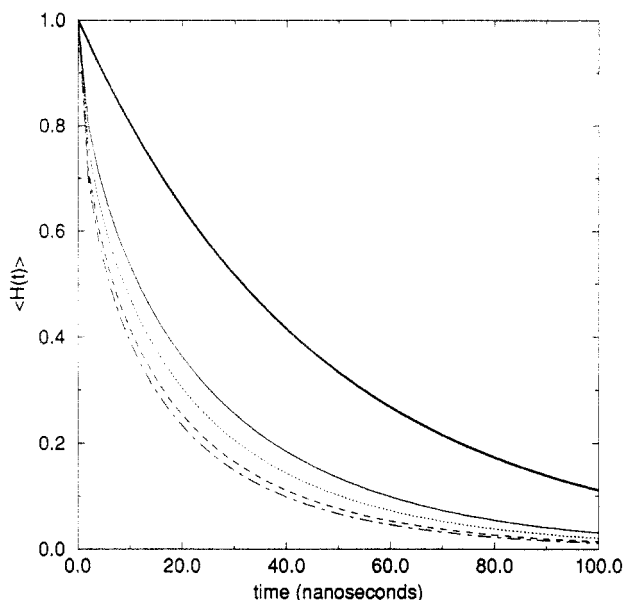


Figure 2. Predicted fluorescence intensity decay with time calculated for varying trap to donor ratio, A , for an end-labeled polyisoprene melt, $N = 1321$ (MW = 90 000), donor = phenanthrene, trap = anthracene: (—) $A = 0$ (no traps), (—) $A = 1$, (···) $A = 2$, (---) $A = 5$, (- - -) $A = 10$.

eters for a donor/trap system of phenanthrene and anthracene where the lifetime of the donor of 45.6 ns is used. Distinguishing between donor-labeled and trap-labeled chains allows variation in A , a parameter that is often changed for optimum energy transfer. This distinction also proves important in describing a system that contains unlabeled polymer.

The correlation function calculated as outlined in Appendix A is for a melt where each polymer chain is end-labeled with a donor or a trap chromophore. By modifying this approach to account for the presence of unlabeled polymer, an additional term is added to adjust for the fact that the chemical procedure used to end-label is often not 100% efficient. The efficiency of end-labeling polyisoprene with chromophores has been reported as ranging from 11 to 85%,^{7,8} while that of end-labeling polystyrene has been reported as 13–100%.^{24,44–47} For systems with relatively low labeling, this can be an

important correction.

The method used to calculate this correlation function is exactly that used to calculate the correlation function for a system of donor- and trap-labeled polymer described in Appendix A, except now there is an additional component in the system, unlabeled polymer. Designating the amount of unlabeled polymer " ρ_U ", the result for a melt of monodisperse polymer is identical to eq 15 with a correction to the coefficient describing the amount of donor- and trap-labeled polymer: $(\rho_T\rho_D/(\rho_T + \rho_D)) \rightarrow (\rho_T\rho_D/(\rho_T + \rho_D + \rho_U))$. (While this correction is essentially what is expected intuitively, it is nonetheless important that it can be proved correct mathematically.) This expression is simplified by letting $\rho_T/\rho_D = A$ and incorporating the fractional efficiency of trap-labeling, T , and donor-labeling, D , into the definitions of ρ_T , ρ_D , and ρ_U . Now $\rho_D \sim (D/(A+1))(1/N)$, $\rho_T \sim (AT/(A+1))(1/N)$, and $\rho_U \sim (1/N)[(1-D) + (1-T)A]/(A+1)$. Substituting in, the donor/trap term can be written ATD/N . Using this straightforward correction, the parameters of any real experimental system can be accurately described by the theoretical model.

C. Semidilute Solution. While the simplest case to treat theoretically is that of a monodisperse melt, solution studies are much more accessible experimentally. Solution studies require that the correlation function calculation includes the changes in the statistics due to the presence of the solvent. In a melt, the chains overlap on all length scales; the chain is modeled as a random walk. In semidilute solution, the chains interpenetrate up to a length scale ξ . For distances smaller than the distance between contacts, ξ , excluded-volume effects cause the chains to swell as compared to random-walk statistics. Following de Gennes' arguments,⁴⁸ the system can be described as a melt of "blobs" of size ξ . Inside each blob, for $r < \xi$, excluded-volume effects must be considered and self-avoiding-walk statistics apply. On larger length scales, for $r > \xi$, the semidilute solution may be considered a random walk of blobs and described with Gaussian statistics. In the calculation of $h_{DT}(r)$ and $h_{DD}(r)$, the Fourier transform integral (eq 13) is split into two parts; instead of integrating with respect to k from 0 to Λ , the integration is done from 0 to $2\pi/\xi$ using the form of the correlation function derived using Gaussian statistics and then from $2\pi/\xi$ to Λ using the asymptotic form of the correlation function for a polymer in good solvent.⁴⁸ (See Appendix B.)

The resulting expression for the correlation function is an extension of eq 15, taking into account both the blob size and the swollen nature of the chain:

$$h_{DT}(r) = \frac{-1}{\pi^2 r} \left(\frac{\rho_T \rho_D}{\rho_T + \rho_D} \right) \left[\left\{ \frac{\pi}{2R_g^2} (\exp(-2^{1/2} r/R_g) - 1) + \frac{\xi}{2\pi r R_g^2} \left[\cos\left(\frac{2\pi r}{\xi}\right) - 1 \right] \right\} + \frac{1}{(2\pi)^{2/3} R_g^{5/3} r} \left\{ \xi^{2/3} \left(\cos\left(\frac{2\pi r}{\xi}\right) - 1 \right) - l^{2/3} \left(\cos\left(\frac{2\pi r}{l}\right) - 1 \right) \right\} \right] \quad (16)$$

If eq 16 is examined in the limit of $\xi \rightarrow l$, the underlined terms cancel, and the semidilute solution correlation function will be equal to that of the melt. (See eq B.3 and Appendix B.) By using a few simple approximations, an expression for $H(t)$ can be found, integrating $h_{DT}(r)$ and $h_{DD}(r)$ over all r as in eq 10. By redefining variables in terms of volume fraction of polymer in solution, ϕ , the donor fluorescence intensity decay for varying polymer solution concentrations can be predicted. de Gennes'⁴⁸ expressions for $R_g(\phi)$ and $\xi(\phi)$ are used; for medium to high molecular weight polymer chains, i.e., for large N , ξ

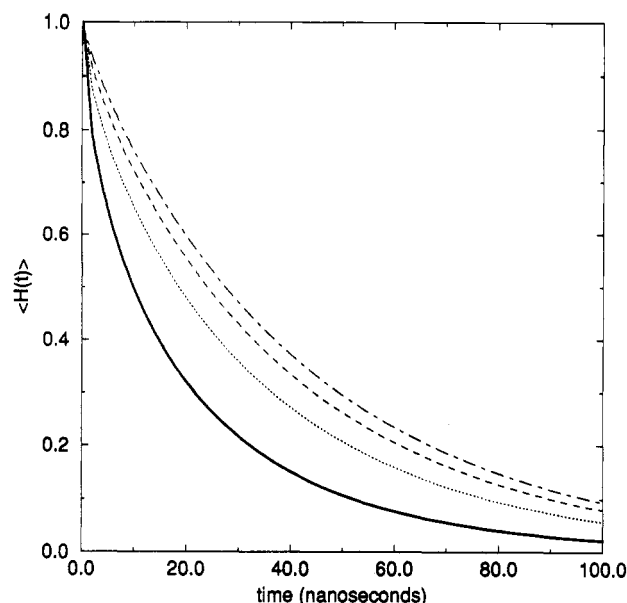


Figure 3. Fluorescence intensity decay with time calculated for varying volume fraction of polymer in solution, ϕ , for an ideal system with perfect end labeling. $N = 1321$ (MW = 90 000), $A = 2$, donor = phenanthrene, trap = anthracene: (—) $\phi = 1.0$, (...) $\phi = 0.4$, (---) $\phi = 0.2$, (- - -) $\phi = 0.1$. The predicted lifetime τ_{pred} is 21.6 ns for ϕ for 1.0 and 42.3 ns for $\phi = 0.1$ assuming $\tau_d = 45.6$ ns.

is only a function of ϕ and not of molecular weight. The donor fluorescence intensity decay is predicted to be affected by solution concentration. (See Figure 3.) As the concentration of the solution is decreased from $\phi = 1.0$ (bulk) to $\phi = 0.1$ for solutions of 90 000 MW anthracene- and phenanthrene-end-labeled polyisoprene, the donor fluorescence lifetime increases, i.e., the decay is slower, which is consistent with reduced energy transfer. A similar effect is predicted for a melt when the molecular weight of the polymer is varied. Figure 4 illustrates the change in the decay profile with molecular weight. Assuming each chain is labeled with one donor or one acceptor, if the chain length, N , is reduced, the overall number of chromophores will increase, leading to increased energy transfer and a shorter fluorescence lifetime.

Experimental Section

Polyisoprene was synthesized by anionic polymerization in sealed glass reactor vessels with a N_2 atmosphere using HPLC-grade cyclohexane (Aldrich) as the solvent and *sec*-butyllithium as the initiator. Prior to being used in synthesis, the cyclohexane was refluxed under a N_2 atmosphere for several days and then refluxed for several more hours after the addition of *sec*-butyllithium as a water scavenger. Isoprene monomer (Aldrich) was treated with dibutylmagnesium and then vacuum-distilled to remove water and impurities prior to polymerization. Identical polymerization reactions were carried out in two different sealed reactor vessels so that material could be easily labeled with either anthracene or phenanthrene.

Polyisoprene was terminally labeled with anthracene or phenanthrene by reacting the living polymer with either 9-(chloromethyl)anthracene (Aldrich) or 9-(bromomethyl)phenanthrene (Molecular Probes). The desired label compound was placed in a sealed glass reactor vessel under a N_2 atmosphere. A small amount (~ 30 mL) of purified cyclohexane, treated in the same manner as that used in synthesis, was added to the reactor vessel to dissolve the label. After the polymerization reactions had been allowed to run for 18 h, the terminating solutions were injected into the reactor vessels containing the living polymer.

Following synthesis, the polyisoprene was precipitated in acetone. To remove the unreacted fluorescent label, the polymer was then cleaned by repeated dissolution in dichloromethane followed by precipitation in acetone. M_n was determined to be 90 000 for both the phenanthrene- and anthracene-labeled

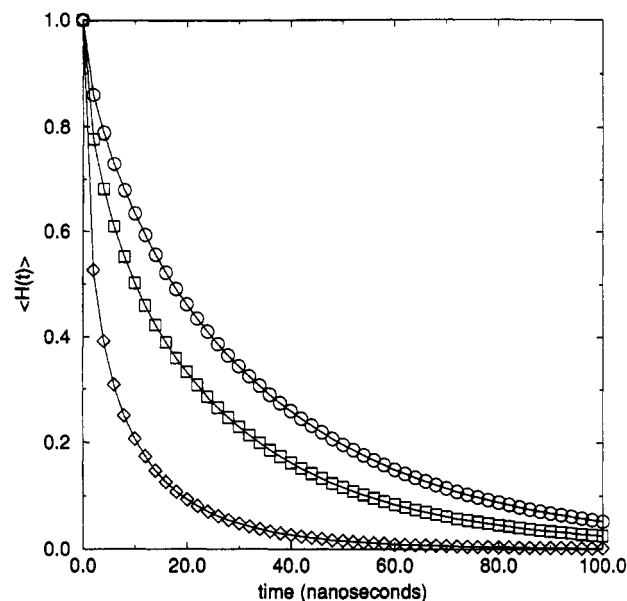


Figure 4. Fluorescence intensity decay with time calculated for bulk polymer ($\phi = 1.0$) for varying N (varying MW) and $A = 2$; (O) $N = 3000$, (□) $N = 1500$, (◇) $N = 500$. Perfect end labeling is assumed.

polymers using gel permeation chromatography as compared to polyisoprene standards (Pressure Chemical). The polydispersity was < 1.2 .⁴⁹ The end-labeling efficiency was determined by UV-vis absorbance spectroscopy to be 70% for phenanthrene and 50% for anthracene. Absorbance measurements were performed with an IBM UV-vis 9410 double-beam spectrophotometer on solutions of labeled polymer in spectrophotometric-grade cyclohexane. Extinction coefficients of model compounds, 9-methylanthracene ($\epsilon_{366 \text{ nm}} = 9600 \text{ M}^{-1} \text{ cm}^{-1}$) and 1-methylphenanthrene ($\epsilon_{299 \text{ nm}} = 15\,500 \text{ M}^{-1} \text{ cm}^{-1}$) were used for comparison. The absorbance spectra of the attached chromophores were red-shifted by 2–3 nm compared to the small-molecule analogs.

Polymer solutions used for donor fluorescence lifetime measurements were prepared in toluene and allowed to sit for 12–24 h to insure complete mixing and dissolution. The solutions were then deoxygenated via five freeze-pump-thaw cycles and blanketed with N_2 prior to experimentation. Small-molecule solutions were prepared and deoxygenated in an identical manner.

Fluorescence lifetimes were measured using time-correlated single photon counting (TC-SPC) on a Photon Technology Inc. TC-SPC system. An excitation wavelength of 299 nm was used, and emission was monitored at 352 nm to measure the phenanthrene lifetime. This emission wavelength was chosen as there is negligible anthracene fluorescence at 352 nm observed in steady-state fluorescence. Data were collected to 10 000 counts in the peak channel over fluorescence decay times of at least 150 ns and analyzed using iterative reconvolution and an iterative fitting procedure to determine the decay profile and the fluorescence lifetimes. The quality of the fit of the data was determined by χ^2 (where $\chi^2 \leq 1.3$ is considered a good fit⁵⁰), the distribution of the weighted residuals, the autocorrelation of the residuals, the Durbin-Watson parameter^{50,51} and the runs test parameter z ⁵² where $z > -1.96$ is a good fit.

Results and Discussion

A. Photophysics of End-Labeled Polymer. Before considering the effects of NRET on donor fluorescence lifetimes, the specific photophysics of the system must be discussed. The absorbance spectra of the labeled polymer were red-shifted 2–3 nm compared to the spectra of the small-molecule analogs. Slight shifts in fluorescence peaks are observed in steady-state experiments as well. Since neither the absorbance nor fluorescence of the attached donor and trap chromophores are identical to those of the small-molecule analogs, the value for the Förster radius for donor-trap NRET, R_0^{DT} , was experimentally verified.

The Förster radius R_0 may be calculated from the following equation:⁵³

$$R_0^6 = \frac{9000\kappa^2\Phi_d \ln 10}{128\pi^5 n^4 N_A} \int \frac{F_d(\nu)\epsilon_a(\nu)}{\nu^4} d\nu \quad (17)$$

where ν is the wavenumber in cm^{-1} , $\epsilon_a(\nu)$ is the molar extinction coefficient of the acceptor in $\text{M}^{-1}\text{cm}^{-1}$, F_d is the fluorescence intensity of the donor normalized to unity such that $\int F_d d\nu = 1$, N_A is Avogadro's number, n is the refractive index of the solvent, Φ_d is the fluorescence quantum yield of the donor, and κ^2 is an orientation factor assumed to be equal to $2/3$. The integral in eq 17 may also be written in terms of the wavelength, λ , as $\int F_d(\lambda)\epsilon_a(\lambda)\lambda^4 d\lambda$.⁵⁴

The absorbance of the anthracene-labeled polyisoprene in a cyclohexane solution was measured as described in the Experimental Section. The fluorescence intensity of the phenanthrene-labeled polyisoprene in a cyclohexane solution was measured via steady-state fluorescence with a SPEX Fluorolog spectrophotometer in the corrected mode using an excitation wavelength of 299 nm. Absorbance of the anthracene-labeled material and the fluorescence intensity of the phenanthrene-labeled material were measured over a range of 340–400 nm where anthracene absorbance and phenanthrene fluorescence overlap. Calculations of R_0^{DT} using data obtained in this manner yielded a Förster radius of 22.4 Å. This is within 3% of the Förster radius reported for phenanthrene and anthracene⁵³ and is considered to be consistent within experimental error.

Having experimentally verified R_0^{DT} for the phenanthrene- and anthracene-labeled polyisoprene, it is also necessary to measure the fluorescence lifetime of the phenanthryl label when it is attached to the end of the polymer chain. The comparison of lifetimes reported for small-molecule phenanthrene of 56–57.5^{55,56} to 44–45.5 ns^{15,22,23,46} reported for randomly phenanthrene-labeled polymer and phenanthrene-labeled block copolymer suggests that chemical attachments can affect the decay behavior of the chromophore. While single-exponential decay behavior has been observed for randomly phenanthrene-labeled poly(butyl methacrylate)²² and poly(methyl methacrylate),²³ experimentally measured donor fluorescence intensity decays for phenanthrene-end-labeled polyisoprene (PI-P) solutions in toluene in the absence of trap in this study did not give a good fit to a single exponential. This is consistent with non-single-exponential decay behavior observed in a variety of end-labeled polymer solutions⁷ and films^{21b} and is likely to be associated with differences in the synthetic procedures for chromophore attachment. It may also be associated with a very small amount of higher molecular weight coupled material present in the system⁴⁹ as well as the lower label content in end-labeled systems as compared to randomly-labeled systems. (Decays measured on dilute solutions of 1-methylphenanthrene in toluene at concentrations $< 5 \times 10^{-4}$ mol/L generally cannot be fit successfully to a single exponential.) Fluorescence intensity decay measurements of 1-methylphenanthrene and phenanthrene end-labeled polyisoprene in toluene can be seen in Figures 5 and 6. The lifetime of 1-methylphenanthrene was determined to be 46.0 ns. While the decay behavior observed from PI-P could not be adequately fit to a single exponential, a biexponential fit yielded a long component lifetime τ_1 of 45.6 ns which is in excellent agreement with τ 's reported for labeled polymer.^{15,22,23,46} Because of this agreement

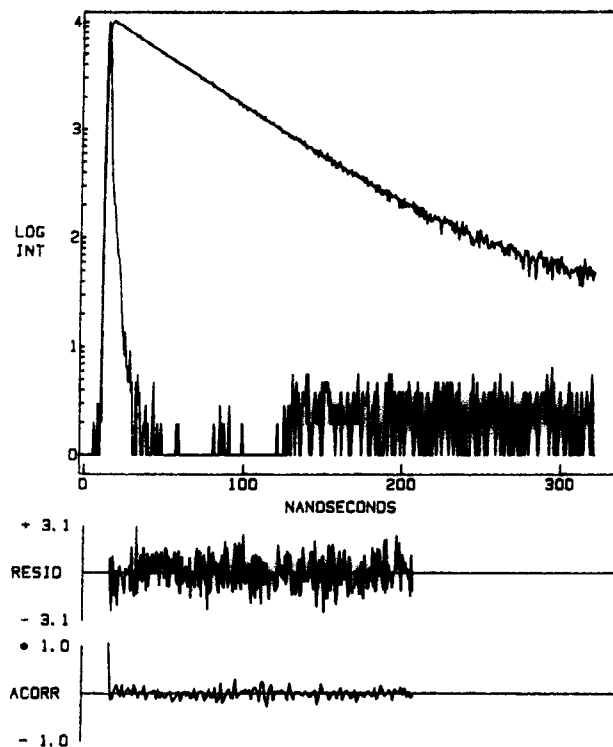


Figure 5. Experimental decay curve for 1-methylphenanthrene in toluene, log (intensity decay) vs time for conc = 5×10^{-4} mol/L: $\alpha_1 = 1.000 \pm 0.054$, $\tau_1 = 46.138 \pm 0.090$. $\chi^2 = 1.120$, DW = 2.127, $z = 0.011$. Measurement taken using TC-SPC, $\lambda_{\text{ex}} = 299$, $\lambda_{\text{em}} = 352$.

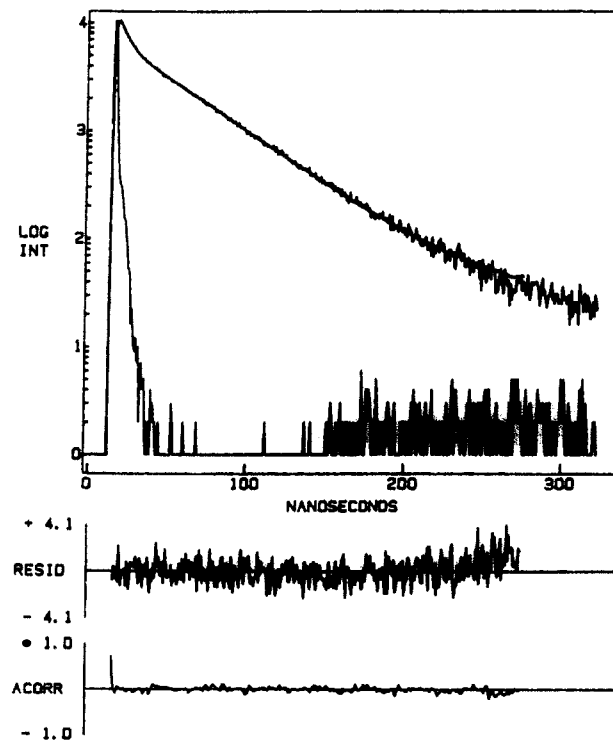


Figure 6. Experimental decay curve for PI-P in toluene, log (intensity decay) vs time for $\phi = 0.253$: $\alpha_1 = 0.440 \pm 0.002$, $\tau_1 = 45.613 \pm 0.102$; $\alpha_2 = 0.560 \pm 0.010$, $\tau_2 = 4.854 \pm 0.108$. $\chi^2 = 1.181$, DW = 1.973, $z = -1.216$. Measurement taken using TC-SPC, $\lambda_{\text{ex}} = 299$, $\lambda_{\text{em}} = 352$.

among the long component of the lifetime τ_1 , the lifetime of the small-molecule analog, and the lifetimes observed for other labelled polymer systems,^{15,22,23,46} we believe that it is this long component lifetime that is of physical significance. Theoretical predictions for specific experimental systems will be compared to experimentally measured τ_1 's in the next section.

B. NRET and Fluorescence Lifetimes. The effects of NRET between the donor and trap are evident in donor fluorescence lifetime measurements as a reduction in the lifetime of the donor, τ_d , compared to that in the absence of acceptors or traps, τ_0 ; the donor is losing some of its excited-state energy through nonradiative energy transfer to the trap rather than returning to the ground state through fluorescence. Experimentally, this is evident in both solutions of unattached donor and trap chromophores and donor- and trap-labeled polymer systems, regardless of labeling geometry. The theoretical predictions of the model are qualitatively consistent with this effect as is illustrated in Figures 2–4. In order to more easily facilitate simple, quantitative comparisons of theory to experiment, it is useful to approximate the theoretically predicted normalized donor fluorescence intensity, $\langle H(t) \rangle$, as a single-exponential decay, resulting in an approximate, corresponding predicted donor fluorescence lifetime, τ_{pred} . The theoretical decays in Figure 3 were calculated for various volume fractions of polymer in solution, ϕ , assuming a system of 90 K polyisoprene ($N = 1321$) end-labeled with anthracene as the trap and phenanthrene as the donor. On the basis of donor fluorescence lifetime of $\tau_0 = 45.6$ ns, Förster radii of $R_0^{\text{DT}} = 22.4$ Å and $R_0^{\text{DD}} = 8.77$ Å,⁵² and a fixed trap-to-donor ratio $A = 2$ and assuming the ideal case of perfect donor and trap-labeling, the donor lifetime is predicted to decrease from 42.3 ns for $\phi = 0.1$ to 33.7 ns for $\phi = 0.4$ and then drop further to 21.6 ns for $\phi = 1.0$ (bulk). As the concentration of the solution increases, the donor-trap correlations change due to increased interactions between the polymer chains as well as an increased amount of chromophores in the system. The change in τ_{pred} reflects increased energy transfer due to changes in the system.

For the case of $\phi = 0.1$ depicted in Figure 3, assuming a solution of perfectly end-labeled material with a 2:1 trap-to-donor ratio, it is significant that only a small reduction in the donor lifetime is predicted. While τ_0 , the lifetime of donor in the absence of any trap, is assumed to be 45.6 ns, τ_{pred} for $\phi = 0.1$ is calculated to be 42.3 ns, a 7% reduction, even though this solution is well within the semidilute regime. A change of this magnitude allows us to quantify more accurately the limitations of the model. Obviously, NRET is very sensitive to the amount of label present in the system. A system of end-labeled polymer is, by definition, fairly dilute in chromophore content since there is only one label per N monomers. Therefore, efficient labeling is crucial for experimentation on higher molecular weight polymers. Lower molecular weight end-labeled polymer systems will exhibit much more significant reductions in donor fluorescence lifetimes than higher molecular weight end-labeled polymer systems at the same concentrations. This effect is observed in Figure 4 which shows the donor fluorescence intensity decay profiles for homopolymer melts of varying molecular weights using a fixed trap/donor ratio ($A = 2$) and using $\tau_0 = 45.6$ ns. The donor fluorescence lifetime is expected to decrease from 32.5 to 23.3 to 6.7 ns as the number of repeat units is decreased from $N = 3000$ to 1500 to 500, consistent with increased energy transfer due to an increased number of chromophores in the system. However, the smaller changes in donor fluorescence lifetimes predicted as a function of solution concentration necessitate precise measurements of the donor fluorescence intensity decay.

The donor fluorescence intensity decays for mixed PI-P and PI-A solutions were measured as a function of polymer concentration and trap-to-donor ratio for five different solutions. Each solution contained a fixed volume fraction of PI-P where $\phi_{\text{PI-P}} \approx 0.253$ so that, as PI-A was added, the solution concentration and the trap-to-donor ratio

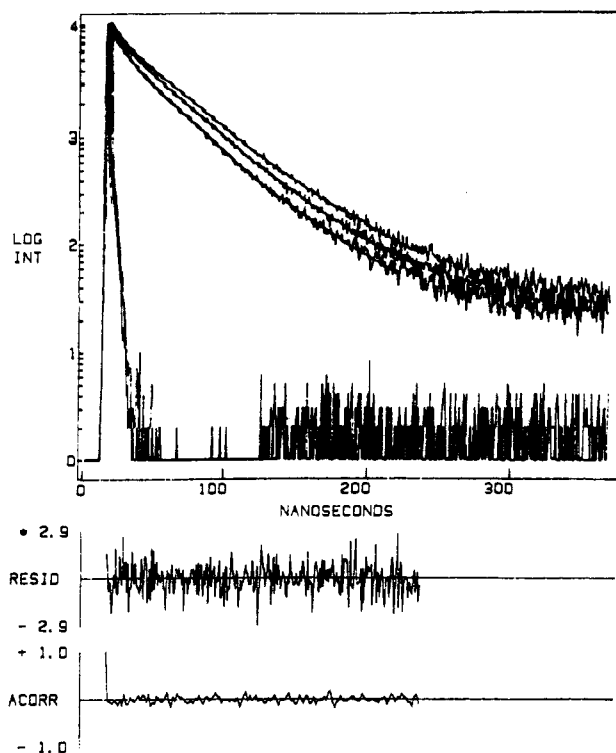


Figure 7. Experimental decay curves for PI-P and PI-A in toluene, log (intensity decay) vs time, $\phi_{\text{PI-P}}$ held constant at $\phi_{\text{PI-P}} = 0.253$: (top decay) measured for $\phi = 0.425$, $A = 0.47$, $\alpha_1 = 0.458 \pm 0.014$, $\tau_1 = 42.023 \pm 0.166$; $\alpha_2 = 0.542 \pm 0.083$, $\tau_2 = 7.886 \pm 0.322$, $\chi^2 = 0.961$, DW = 1.791, $z = 0.665$; (middle decay) measured for $\phi = 0.5$, $A = 0.7$, $\alpha_1 = 0.347 \pm 0.008$, $\tau_1 = 40.392 \pm 0.159$; $\alpha_2 = 0.653 \pm 0.092$, $\tau_2 = 7.028 \pm 0.302$, $\chi^2 = 1.060$, DW = 1.867, $z = -0.679$; (bottom decay) measured for $\phi = 0.55$, $A = 0.84$, $\alpha_1 = 0.372 \pm 0.013$, $\tau_1 = 38.831 \pm 0.197$; $\alpha_2 = 0.628 \pm 0.041$, $\tau_2 = 10.144 \pm 0.335$, $\chi^2 = 1.148$, DW = 2.050, $z = 1.696$. Distribution of the weighted residuals and autocorrelation of the residuals shown is for the $\phi = 0.425$ curve. Measurements taken using TC-SPC are $\lambda_{\text{ex}} = 299$ and $\lambda_{\text{em}} = 352$.

increased. In each case, the decay could be fit to a biexponential form; however, as with the decay for PI-P, there is no reason to believe that a double-exponential fit has any particular photophysical significance. As solution concentration and trap-to-donor ratios were increased, the long component of the lifetime τ_1 steadily decreased, consistent with the effects of NRET and with the predictions of the model.⁵⁷ Representative experimental decay curves are given in Figure 7. For purposes of comparison of experiment to theory, normalized donor fluorescence intensity decays, $\langle H(t) \rangle$, were calculated using the parameters of the experimental system including polymer molecular weight (for 90 000 polyisoprene, $N = 1321$), donor and trap label content (including label efficiency), volume fraction of polymer in solution, and the experimentally measured τ_1 for PI-P = 45.6 ns. A comparison of the predicted lifetimes τ_{pred} and the experimentally measured τ_1 's is given in Table I. Clearly, the results for $\tau_{1(\text{exp})}$ are in excellent quantitative agreement with the values determined by the model. Whereas the overall experimental changes in solution concentration and in the trap/donor ratio are not dramatic and lead to predictions of relatively small reductions in donor lifetime, the technique has proved sensitive to changes of this magnitude. The ability to measure these lifetimes precisely is still crucial, especially when only small changes are expected, but the sensitivity of the TC-SPC technique and the theoretical model to specific experimental parameters demonstrated here is an important step in using fluorescence NRET techniques in a more quantitative manner.

Table I. Predicted and Experimental Excited-State Donor Lifetimes^a

φ	n_T/n_D	τ_{pred} (ns)	$\tau_{1(\text{exp})}$ (ns)
0.300	0.133	44.32	44.39 \pm 0.14
0.350	0.275	43.32	43.25 \pm 0.14
0.425	0.470	41.87	42.02 \pm 0.17
0.500	0.700	40.26	40.39 \pm 0.16
0.550	0.840	39.25	38.83 \pm 0.20

^a Results are for solutions of PI-A (50% labeling) and PI-P (70% labeling) in toluene, MW = 90 000 ($N = 1321$), $\tau_{1(\text{exp})} = 45.6$ ns. τ_{pred} was determined by approximating calculated $\langle H(t) \rangle$ for each system as a single-exponential decay. Experimental donor fluorescence decays measured using TC-SPC.

Conclusions

A relationship between donor fluorescence intensity decay and the donor-trap correlation function in a melt of end-labeled monodisperse polymer has been determined. Relevant chain statistics and intermolecular interactions have been included in the model. The arguments have been extended to describe donor fluorescence intensity decay in semidilute solutions. While the problems of the polymer melt and the solution are treated in a self-consistent manner, the swollen nature of the chain in solution is accounted for in the determination of the correlation function rather than merely incorporating solution concentration into the final expression for $\langle H(t) \rangle$. The model has been further extended to describe a real experimental donor- and trap-end-labeled system where end labeling is not ideal. Such a model should be accessible to experimentalists since it includes all relevant experimental parameters.

Theoretical predictions for a semidilute solution indicate that the normalized donor fluorescence intensity decay $\langle H(t) \rangle$ should scale with the polymer volume fraction in solution, φ . Experimental results from fluorescence lifetime measurements are in good agreement with the theory even in the limiting case of low label content polymer in a semidilute solution. Since φ is a function of blob size ξ , it is possible that fluorescence techniques could be used to investigate the blob size in solution and perhaps also chain statistics in other systems.

This is the first study to make a direct quantitative comparison between a theoretical model including correlations in solution and fluorescence lifetime measurements. Although relatively simple systems have been examined here, this model provides a base on which to study systems with more complicated statistics. Work is currently underway investigating bimodal blends where the donor- and trap-labeled chains are chemically identical but of different molecular weights.⁴¹ For sufficiently short lower molecular weight chains, the higher molecular weight chains in a bimodal blend have been shown to be expanded relative to random-walk statistics even in the melt state.^{58,59} Further, while the work described here has assumed that all interaction terms are zero, χ terms have been included in the calculation of the correlation function (see Appendix A). Thus, through appropriate inclusion of interaction terms, this model could be applied to miscible blends of unlike polymer.⁶⁰ While the present study has demonstrated that correlations in monodisperse polymer solutions can be investigated by quantitative comparison of fluorescence theory and experiments, extensions of the model to polydisperse or blend systems could make fluorescence a competitive alternative to scattering techniques generally used to study chain statistics.

Acknowledgment. The authors thank Professor P. W. Voorhees and A. Dhinojwala for useful discussions. This work was supported by NSF Grant DMR-9057764

and by the David & Lucile Packard Foundation. We also acknowledge support from the AAUW Educational Foundation in the form of a Selected Professions Fellowship (A.S.M.).

Appendix A: Calculation of the Correlation Function

In order to find the Fourier transform of the correlation function $h(r) = \langle \rho_k^i \rho_{-k}^i \rangle$, the probability functional $P[\{\rho_k\}]$ must be constructed. The basic procedure to obtain the probability functional is the same as that used by Olvera de la Cruz, Edwards, and Sanchez⁴³ to calculate the probability functional for a monodisperse blend of polymers A and B. To extend their arguments to the case of a system of donor- and trap-labeled polymer, we impose the additional constraint that the chains of A and B are chemically linked. This is the same constraint used to determine the probability functional for a block copolymer. Next, the A-B chain is examined in the limit where one of the blocks is only one unit long. This is the case of end-labeled homopolymer.

The partition function for a polymer blend contains a Gaussian distribution of A monomers for each A chain, a Gaussian distribution of B monomers for each B chain, the thermodynamic interactions between A chains and B chains, and the constraint of incompressibility (there are no "holes" in the melt). Following the notation and arguments used by Olvera de la Cruz et al.,⁴³ the probability distribution is

$$P[\{R_{\alpha_i}\}] = \exp \left\{ - \sum_{i,j} \left(\frac{3}{2l_i} \right) \sum_{\alpha_i} \int ds_{\alpha_i} \left(\frac{dR_{\alpha_i}}{ds} \right)^2 \right\} \exp[-U[\{R_{\alpha_i}\}]/kT] \quad (\text{A.1})$$

where the first exponential term describes Gaussian statistics and the second term includes the short-range interactions, w_{ij} , between monomers:

$$U[\{R_{\alpha_i}\}] = \sum_{i,j} \sum_{\alpha_i} \sum_{\alpha_j} w_{ij} \int \frac{ds_{\alpha_i}}{l_i} \int \frac{ds_{\alpha_j}}{l_j} \delta[R_{\alpha_i}(s_{\alpha_i}) - R_{\alpha_j}(s_{\alpha_j})] \sum_{i,j} w_{ij} \int \rho_i(r) \rho_j(r) d^3r \quad (\text{A.2})$$

where $\rho_i(r)$ is the microscopic density of monomers

$$\rho^i(r) = \sum_{\alpha_i} \int \frac{ds_{\alpha_i}}{l_i} \delta(r - R_{\alpha_i}) \quad i = A, B \quad (\text{A.3})$$

The partition function, Z , is then obtained by integrating $P[\{R_{\alpha_i}\}]$ over all possible configurations, using the incompressibility constraint:

$$Z = \prod_{i=A,B} \int \prod_{\alpha_i} \delta R_{\alpha_i} P[\{R_{\alpha_i}\}] \delta(\varphi_A(r) + \varphi_B(r) - 1) \quad (\text{A.4})$$

where the incompressibility constraint is $\varphi_A(r) + \varphi_B(r) = 1$, rewritten in the form of a delta function. Using the definition of the mean density,

$$\rho_0^i = \frac{1}{V} \int d\mathbf{r} \rho^i(r) = n_i N_i / V \quad (\text{A.5})$$

we can rewrite $\varphi_A(r)$ and $\varphi_B(r)$ in terms of $\rho^i(r)$:

$$\varphi_A(r) = \rho^A(r)/\rho, \quad \varphi_B(r) = \rho^B(r)/\rho \quad (\text{A.6})$$

where $\rho = \rho_0^A + \rho_0^B$ = total mean density.

To calculate the effect of concentration fluctuations, the probability distribution is expressed in terms of the Fourier components of $\rho^i(\mathbf{r})$:

$$\rho_k^i = \frac{1}{V} \sum_{\alpha_i} \int \frac{ds_{\alpha_i}}{l_i} \exp[i\mathbf{k} \cdot \mathbf{R}_{\alpha_i}(s_{\alpha_i})] \quad (\text{A.7})$$

ρ_0^i is the average density of the i th component, so ρ_k^i for $k \neq 0$ denotes local concentration fluctuations. Using the Fourier components, the incompressibility constraint may be rewritten $\prod_{k \neq 0} \delta(\rho_k^A + \rho_k^B) \delta(\rho_0^A + \rho_0^B - \rho)$ as can the energy term in eq A.2: $U[\{\rho_k^i\}]/kT = \sum_{i,j} \frac{V w_{ij}}{2kT} \sum_k \rho_k^i \rho_k^{j*}$ where $\rho_k^{i*} = \rho_{-k}^i$ (the complex conjugate).

To rewrite the probability functional in terms of the local fluctuations ρ_k^i , Z must be multiplied by the Jacobian of the transformation:

$$\prod_{i=A,B} \int \prod_k d\rho_k^i \delta \left\{ \rho_k^i - \frac{1}{V} \sum_{\alpha_i} \int \frac{ds_{\alpha_i}}{l_i} \exp[i\mathbf{k} \cdot \mathbf{R}_{\alpha_i}(s_{\alpha_i})] \right\} \quad (\text{Jacobian})$$

or equivalently

$$\prod_{i=A,B} \int \prod_k d\rho_k^i \int \frac{d\lambda_k^i}{2\pi} \exp \left[i\lambda_k^i \left\{ \rho_k^i - \frac{1}{V} \sum_{\alpha_i} \int \frac{ds_{\alpha_i}}{l_i} \exp[i\mathbf{k} \cdot \mathbf{R}_{\alpha_i}(s_{\alpha_i})] \right\} \right] \quad (\text{A.8})$$

The entire partition function is then expressed by substituting eqs A.1 and A.2 into eq A.4, using the incompressibility constraint in terms of ρ_k^i , and the Jacobian in the parametrized form (eq A.8). (See eq 23, ref 43.)

From this point, the partition function is simplified by integrating the Gaussian distribution terms, and Z is rewritten using matrices, where Z_0 contains all the $k = 0$ terms:

$$Z = Z_0 \int \prod_{i=A,B} d\rho_k^i \frac{d\lambda_k^i}{2\pi} \exp \left\{ \frac{-1}{2V} \sum_{k \neq 0} (\lambda_k^A \lambda_k^B) \mathbf{A} \begin{pmatrix} \lambda_{-k}^A \\ \lambda_{-k}^B \end{pmatrix} + i \sum_{k \neq 0} (\rho_k^A \rho_k^B) \begin{pmatrix} \lambda_{-k}^A \\ \lambda_{-k}^B \end{pmatrix} \right\} \exp[-U[\{\rho_k^i\}]/kT] \delta(\rho_k^A + \rho_k^B) \quad (\text{A.9})$$

where \mathbf{A} is a 2×2 matrix equal to

$$\mathbf{A} = \begin{bmatrix} n_A D_A(k) & 0 \\ 0 & n_B D_B(k) \end{bmatrix} \quad n_A, n_B = \text{no. of A, B chains}$$

$D^i(k)$ is a Debye function, which is the result of an integral of the form

$$D^i(k) = \frac{1}{l^2} \int ds \int ds' \exp \left[-\frac{k^2 l^2}{6} |s - s'| \right] \quad i = A, B \quad (\text{A.10})$$

$$D^i(x_i) = (2N^2/x_i^2)[x_i + e^{-x_i} + 1]$$

where $x_i = k^2 R_{gi}^2$ and R_{gi} is the radius of gyration of the polymer chain, $R_{gi}^2 = N l^2/6$.

From eq A.9, the integration with respect to $d\lambda_k^i$ can be performed. In matrix form the result is expressed in terms of the inverse of \mathbf{A} , \mathbf{A}^{-1} (Z_0 now contains all $k = 0$ terms

as well as all constants):

$$Z = Z_0 \int \prod_{k \neq 0} d\rho_k^A d\rho_k^B \delta(\rho_k^A + \rho_k^B) \times \exp \left\{ \frac{-1}{2V} \sum_{k \neq 0} (\rho_k^A \rho_k^B) (\mathbf{A}^{-1} + \mathbf{W}) \begin{pmatrix} \rho_{-k}^A \\ \rho_{-k}^B \end{pmatrix} \right\} \quad (\text{A.11})$$

where \mathbf{W} is a 2×2 matrix that consists of the interaction terms:

$$\mathbf{W} \sim \frac{1}{kT} \begin{bmatrix} w_{AA} & w_{AB} \\ w_{AB} & w_{BB} \end{bmatrix}$$

Integrating over $d\rho_k^B$, the final result is the simplified partition function:

$$Z = Z_0 \int \prod_{k \neq 0} d\rho_k^A P[\{\rho_k^A\}] = \int \prod_{k \neq 0} d\rho_k^A \exp \left\{ \frac{-1}{2V} \sum_k \frac{\rho_k^A \rho_{-k}^A}{S(k)} \right\} \quad (\text{A.12})$$

where $S(k) = \langle \rho_k^A \rho_{-k}^A \rangle = 1/(1/n_A D_A + 1/n_B D_B - 2\chi)$ and χ is the Flory-Huggins interaction parameter, $\chi = [w_{AB} - (1/2)(w_{AA} + w_{BB})]/kT$.

Following the same mathematical procedure, the partition function for a melt of AB diblock copolymers can be calculated starting from the same point (eqs A.1, A.2, and A.4) with one additional constraint. For a diblock, the A and B chains are chemically linked. This is expressed mathematically with the condition that the end point of the A block is the same as the initial point of the B block, or $r_A(L) = r_B(0)$. In terms of a delta function, this condition becomes $\delta(r_A(L) - r_B(0))$. The same procedure is then followed to simplify the partition function.

In the case of a diblock copolymer, the thermodynamic interactions, described by \mathbf{W} , are identical. The matrix \mathbf{A} that is the result of integrating over the Gaussian part of the chain coupled with the field (see eqs A.9 and A.10), is now different. The off-diagonal terms in \mathbf{A} are now nonzero as the result of the connectivity of the blocks. In the partition function for a diblock copolymer,

$$\mathbf{A} = \begin{bmatrix} n D_A & n D_A^{1/2} D_B^{1/2} \\ n D_A^{1/2} D_B^{1/2} & n D_B \end{bmatrix}$$

where D_A and D_B are the Debye functions from eq A.10, n is the number of polymer chains, and $D_A^{1/2}$ and $D_B^{1/2}$ are what we call "half-Debye functions". The subscripts A and B refer to the A and B blocks, respectively. These functions result from an integral of the type:

$$D_i^{1/2} = \int \frac{ds}{l} \exp \left[-\frac{k^2 l^2}{6} |s - s'| \right] = \frac{N}{x_i} (1 - e^{-x_i})$$

where $x_i = k^2 R_{gi}^2$ as before.

For the case of end-labeled polymer chains, the $D^{1/2}$ and the D term for the "label block" are equal to unity, since we are only integrating over one unit, instead of the whole chain. The matrix \mathbf{A} , describing the connectivity in the system, now reduces to

$$\mathbf{A} = \begin{bmatrix} n D & n D^{1/2} \\ n D^{1/2} & n \end{bmatrix}$$

The results obtained for $\langle \rho_k^l \rho_{-k}^l \rangle$, where l refers to "label", using this value of \mathbf{A} and the partition function described above are essentially equivalent to that of de Gennes.³⁹

For the donor- and trap-labeled polymer system, the distinction between the traps and the donors, and also between the linear chain labeled with traps and the linear chain labeled with donors, must be made. **A** and **W** become 4×4 matrices, and the partition function becomes a slightly more complicated version of eq A.9 (see eq A.13 below). ρ_{lk}^T and ρ_{lk}^D refer to the concentration of the linear portion of the trap- and donor-labeled chains, respectively; σ_k^T and σ_k^D refer to the labels.

$$Z = Z_0 \int \prod_{i=A,B} d\rho_k^i d\sigma_k^i \frac{d\lambda_k^i}{2\pi} \times \exp \left\{ \frac{-1}{2V} \sum_{k \neq 0} (\lambda_{lk}^T \lambda_{lk}^D \lambda_k^T \lambda_k^D) \mathbf{A} \begin{pmatrix} \lambda_{l-k}^T \\ \lambda_{l-k}^D \\ \lambda_{-k}^T \\ \lambda_{-k}^D \end{pmatrix} + i \sum_{k \neq 0} (\rho_{lk}^T \rho_{lk}^D \sigma_k^T \sigma_k^D) \begin{pmatrix} \lambda_{l-k}^T \\ \lambda_{l-k}^D \\ \lambda_{-k}^T \\ \lambda_{-k}^D \end{pmatrix} \right\} \times \exp[-U\{\rho_{lk}^T \rho_{lk}^D \sigma_k^T \sigma_k^D\}/kT] \delta(\rho_{lk}^T + \rho_{lk}^D + \sigma_k^T + \sigma_k^D) \quad (\text{A.13})$$

For this system

$$\mathbf{A} = \begin{bmatrix} n_T D_T & 0 & n_T D_T^{1/2} & 0 \\ 0 & n_D D_D & 0 & n_D D_D^{1/2} \\ n_T D_T^{1/2} & 0 & n_T & 0 \\ 0 & n_D D_D^{1/2} & 0 & n_D \end{bmatrix}$$

and

$$\mathbf{W} = \begin{bmatrix} w_{LL} & w_{LL} & w_{LT} & w_{LD} \\ w_{LL} & w_{LL} & w_{LT} & w_{LD} \\ w_{LT} & w_{LT} & w_{TT} & w_{DD} \\ w_{LD} & w_{LD} & w_{TD} & w_{DD} \end{bmatrix}$$

where the subscripts in the interaction matrix, L, T, and D, refer to "linear" polymer, trap, and donor, respectively.

The partition function is then integrated and simplified in much the same manner as the others described above. We have also made one additional assumption that the concentrations of the donors and traps themselves are very small compared to the concentration of the linear part of the polymer chains; therefore, the incompressibility constraint will reduce to $\delta(\rho_{lk}^T + \rho_{lk}^D)$. This assumption allows us to simply further the 4×4 matrix **B** in the partition function, where **B** = **A**⁻¹ + **W**, to a 3×3 matrix **C**, where $X = D_T - (D_T^{1/2})^2$ and $Y = D_D - (D_D^{1/2})^2$:

$$\mathbf{C} = \begin{bmatrix} \frac{1}{n_T X} + \frac{1}{n_D Y} & \frac{-D_T^{1/2}}{n_T X} & \frac{D_D^{1/2}}{n_D Y} \\ \frac{-D_T^{1/2}}{n_T X} & \frac{D_T}{n_T X} + w_{TT} & w_{TD} \\ \frac{D_D^{1/2}}{n_D Y} & w_{TD} & \frac{D_D}{n_D Y} + w_{DD} \end{bmatrix} \quad (\text{A.14})$$

In doing this, it becomes apparent that the thermodynamic interactions that are relevant are those between the donors and the traps; effectively the system seems to act like a

gas of labels. In most end-labeled systems, however, the concentration of labels is sufficiently low compared to the concentration of monomers that the thermodynamic interactions between labels can be considered negligible.

The correlation function between donors and traps is then calculated, assuming $w_{TT} = w_{DD} = w_{TD} = 0$, where ρ_T and ρ_D refer to the number density of trap-labeled chains and donor-labeled chains, respectively:

$$\langle \sigma_k^T \sigma_{-k}^D \rangle = \frac{-\rho_T \rho_D D_T^{1/2} D_D^{1/2}}{\rho_D D_D + \rho_T D_T} \quad (\text{A.15})$$

This is obtained from eq A.13 and **C**⁻¹ (eq A.16), the inverse of **C**, which contains all the correlation functions in the system. $\langle \sigma_k^D \sigma_{-k}^D \rangle$, the donor-donor correlation function, is equal to c_{33}^{-1} and the trap-trap correlation function is given by c_{22}^{-1} .

$$\mathbf{C}^{-1} = \left(\frac{1}{n_D D_D + n_T D_T} \right) \times \begin{bmatrix} n_T n_D D_T D_D & n_T n_D D_T D_D^{1/2} & -n_T n_D D_T D_D^{1/2} \\ n_T n_D D_D D_T^{1/2} & n_T n_D D_D + n_T^2 X & -n_T n_D D_T^{1/2} D_D^{1/2} \\ -n_T n_D D_T D_D^{1/2} & -n_T n_D D_T^{1/2} D_D^{1/2} & n_T n_D D_T + n_D^2 Y \end{bmatrix} \quad (\text{A.16})$$

Appendix B: Self-Consistent Calculation of $h_{DT}(r)$ for Melt and Semidilute Solutions

Since physical interactions for distances $r < l$ (or in Fourier space, $k > 2\pi/l$) are generally not considered, we can change the limits of integration on eq 14, the correlation function for the melt. Instead of integrating from 0 to ∞ , the limits of integration are 0 to $\Lambda = 2\pi/l$. This is consistent with the manner in which the correlation function for a semidilute solution was calculated. Incorporating the approximation for the Debye function,⁴² the integral then becomes

$$h_{DT}(r) = \frac{-1}{\pi^2 r} \left(\frac{\rho_T \rho_D}{\rho_T + \rho_D} \right) \int_0^\Lambda \frac{k \sin(kr)}{(2 + (kR_g)^2)} dk \quad (\text{B.1})$$

We can solve this integral by considering that eq B.1 is equal to

$$h_{DT}(r) = \frac{-1}{\pi^2 r} \left(\frac{\rho_T \rho_D}{\rho_T + \rho_D} \right) \left\{ \int_0^\infty \frac{k \sin(kr)}{(2 + (kR_g)^2)} dk - \int_\Lambda^\infty \frac{k \sin(kr)}{(2 + (kR_g)^2)} dk \right\} \quad (\text{B.2})$$

The first integral is equivalent to eq 14, employing the approximation for the Debye function.⁴² Assuming that $(kR_g)^2 \gg 2$, the second integral is equivalent to the sine integral,⁶¹ $\text{si}(y)$, where $\text{si}(y) = -\int_y^\infty (\sin t)/t dt = -\pi/2 + \int_0^y (\sin t)/t dt$. If $y \rightarrow \infty$, then $\text{si}(y) = 0$ since $\int_0^\infty (\sin t)/t dt = \pi/2$. In eq B.2 this is when $l \rightarrow 0$; and eq B.1 will equal eq 14. For $l > 0$, $\text{si}(y)$ can be approximated as a convergent infinite series which in turn can be approximated as an analytic function of y . The result of integrating eq B.2 is then

$$h_{DT}(r) = \frac{-1}{\pi^2 r} \left(\frac{\rho_T \rho_D}{\rho_T + \rho_D} \right) \left\{ \frac{\pi}{2R_g^2} [\exp(-2^{1/2}r/R_g)] + \frac{1}{R_g^2} \left[\text{si}\left(\frac{2\pi r}{l}\right) \right] \right\}$$

For $l \rightarrow 0$

$$h_{DT}(r) = \frac{-1}{\pi^2 r} \left(\frac{\rho_T \rho_D}{\rho_T + \rho_D} \right) \left\{ \frac{\pi}{2R_g^2} [\exp(-2^{1/2} r/R_g)] \right\}$$

recovering the correlation function for the melt. For larger l , using the approximation for $si(y)$,

$$h_{DT}(r) = \frac{-1}{\pi^2 r} \left(\frac{\rho_T \rho_D}{\rho_T + \rho_D} \right) \left\{ \frac{\pi}{2R_g^2} [\exp(-2^{1/2} r/R_g) - 1] - \frac{1}{2\pi r R_g^2} \left[\cos\left(\frac{2\pi r}{l}\right) - 1 \right] \right\} \quad (B.3)$$

This is consistent with the manner in which the correlation function for the semidilute solution has been calculated. The integral for $h_{DT}(r)$ for the semidilute solution is split considering Gaussian statistics (RW) outside the blob and self-avoiding walk (SAW) statistics inside the blob: $h(r) = \int_0^{2\pi/\xi} RW + \int_{2\pi/\xi}^{\Lambda} SAW$ where $\int_{2\pi/\xi}^{\Lambda} SAW = \int_{2\pi/\xi}^{\infty} SAW - \int_{\Lambda}^{\infty} SAW$. The resulting correlation function can be again written in terms of $si(2\pi r/\xi)$ and $si(2\pi r/l)$. In the limit of $\xi \rightarrow 1$, eq B.3 is recovered, and for $l \rightarrow 0$, the correlation function for the melt is recovered. The donor-donor correlation function is treated in an identical manner.

References and Notes

- Amrani, F.; Hung, J. M.; Morawetz, H. *Macromolecules* **1980**, *13*, 649.
- Albert, B.; Jerome, R.; Teyssié, P.; Smyth, G.; Boyle, N. G.; McBrierty, V. J. *Macromolecules* **1985**, *18*, 388.
- Mikes, F.; Morawetz, H.; Dennis, K. S. *Macromolecules* **1984**, *17*, 16.
- Albert, B.; Jerome, R.; Teyssié, P. *J. Polym. Sci., Polym. Chem. Ed.* **1987**, *24*, 2577.
- Chang, L. P.; Morawetz, H. *Macromolecules* **1987**, *20*, 428.
- Torkelson, J. M.; Gilbert, S. R. *Macromolecules* **1987**, *20*, 1860.
- Major, M. D.; Torkelson, J. M.; Brearley, A. M. *Macromolecules* **1990**, *23*, 1711.
- Major, M. D.; Torkelson, J. M.; Brearley, A. M. *Macromolecules* **1990**, *23*, 1700.
- Procházka, K.; Bednár, B.; Mukhtar, E.; Svoboda, P.; Trnená, J.; Almgren, M. *J. Phys. Chem.* **1991**, *95*, 4563.
- Wilhelm, M.; Zhao, C.; Wang, Y.; Xu, R.; Winnik, M. A.; Mura, J.; Riess, G.; Croucher, M. D. *Macromolecules* **1991**, *24*, 1033.
- Cao, T.; Munk, P.; Ramireddy, C.; Tuzar, Z.; Webber, S. E. *Macromolecules* **1991**, *24*, 6300.
- Kiserow, D.; Chan, J.; Ramireddy, C.; Munk, P.; Webber, S. E. *Macromolecules* **1992**, *25*, 5338.
- Procházka, K.; Kiserow, D.; Ramireddy, C.; Tuzar, Z.; Munk, P.; Webber, S. E. *Macromolecules* **1992**, *25*, 454.
- Winnik, M. A.; Pekcan, O.; Chen, L.; Croucher, M. D. *Macromolecules* **1988**, *21*, 55.
- Winnik, M. A.; Disanayaka, B.; Pekcan, O.; Croucher, M. D. *J. Colloid Interface Sci.* **1990**, *139*, 251.
- Pekcan, O.; Egan, L.; Winnik, M. A.; Croucher, M. D. *Macromolecules* **1990**, *23*, 2210.
- Pekcan, O.; Winnik, M. A.; Croucher, M. D. *Chem. Phys.* **1990**, *146*, 283.
- Ediger, M. D.; Domingue, R. P.; Peterson, K. A.; Fayer, M. D. *Macromolecules* **1985**, *18*, 1182.
- Liu, C.; Morawetz, H. *Macromolecules* **1988**, *21*, 515.
- Vyprachticky, D.; Morawetz, H.; Fainzilberg, V. *Macromolecules* **1993**, *26*, 339.
- (a) Spangler, L. L.; Torkelson, J. M., submitted for publication. (b) Spangler, L. L. Ph.D. Thesis, Department of Chemical Engineering, Northwestern University, 1992.
- Wang, Y.; Zhao, C.; Winnik, M. A. *J. Chem. Phys.* **1991**, *95*, 2143.
- Pekcan, O.; Winnik, M. A.; Croucher, M. D. *Macromolecules* **1990**, *23*, 2673.
- (a) Gebert, M. S. Ph.D. Thesis, Department of Chemical Engineering, Northwestern University, 1991. (b) Gebert, M. S.; Torkelson, J. M. *Polymer* **1990**, *21*, 2402. (c) Gebert, M. S.; Yu, D. H.-S.; Torkelson, J. M. *Macromolecules* **1992**, *25*, 4160.
- Shiah, T. Y.; Morawetz, H. *Macromolecules* **1984**, *17*, 792.
- Spangler, L. L.; Torkelson, J. M., submitted for publication.
- Lakowicz, J. R.; Wicz, W.; Gryczynski, I.; Fishman, M.; Johnson, M. L. *Macromolecules* **1993**, *26*, 349.
- Henriouille-Granville, M.; Kyuda, K.; Jérôme, R.; Teyssié, P.; De Schryver, F. C. *Macromolecules* **1990**, *23*, 1202.
- Chen, C. T.; Morawetz, H. *Macromolecules* **1989**, *22*, 159.
- Jiang, M.; Chen, W.; Yu, T. *Polymer* **1991**, *32*, 984.
- Pekcan, O.; Winnik, M. A.; Egan, L.; Croucher, M. D. *Macromolecules* **1983**, *16*, 699.
- Förster, T. *Z. Naturforsch., A: Astrophys., Phys. Phys. Chem.* **1949**, *4*, 321.
- Ohmine, I.; Silbey, R.; Deutch, J. M. *Macromolecules* **1977**, *10*, 862.
- Ediger, M. D.; Fayer, M. D. *Macromolecules* **1983**, *16*, 1839.
- Peterson, K. A.; Fayer, M. D. *J. Chem. Phys.* **1986**, *85*, 4703.
- Fredrickson, G. H.; Anderson, H. C.; Frank, C. W. *Macromolecules* **1984**, *17*, 1496.
- Fredrickson, G. H. *Macromolecules* **1986**, *19*, 441.
- Haas, S. W.; Zwanzig, R. *J. Chem. Phys.* **1978**, *68*, 1879.
- de Gennes, P.-G. *J. Phys. (Paris)* **1970**, *31*, 235.
- Nieuwoudt, J.; Mukamel, S. *Phys. Rev. B* **1984**, *30*, 4426.
- Mendelsohn, A. S.; Olvera de la Cruz, M., to be submitted for publication.
- Doi, M.; Edwards, S. F. *The Theory of Polymer Dynamics*; Clarendon Press: Oxford, U.K., 1986.
- Olvera de la Cruz, M.; Edwards, S. F.; Sanchez, I. C. *J. Chem. Phys.* **1988**, *89*, 1704.
- Tang, W. T.; Hadziioannou, G.; Smith, B. A.; Frank, C. W. *Polymer* **1988**, *29*, 1718.
- Quirk, R. P.; Schock, L. E. *Macromolecules* **1991**, *24*, 1237.
- Ni, S.; Juhué, D.; Moselhy, J.; Wang, Y.; Winnik, M. A. *Macromolecules* **1992**, *25*, 496.
- Mita, I.; Horie, K.; Takeda, M. *Macromolecules* **1981**, *14*, 1428.
- de Gennes, P.-G. *Scaling Concepts in Polymer Physics*; Cornell University Press: Ithaca, NY, 1979.
- The gel permeation chromatograms for the end-labeled polyisoprenes synthesized here exhibit very small high molecular weight shoulders. Without these shoulders, the polydispersities measured are ≤ 1.1 . This phenomenon has also been observed for end-labeled polystyrenes and block copolymers synthesized in our laboratory. We believe this shoulder may be indicative of a very small degree of coupling between living polymer chains upon the addition of the reactive label compound.
- O'Connor, D. V.; Phillips, D. *Time-Correlated Single Photon Counting*; Academic Press: London, 1984.
- According to ref 50, if the Durbin-Watson parameter, DW, is greater than 1.7 or 1.75 for a single- or double-exponential decay, respectively, then a good fit has been achieved.
- Hamburg, M. *Basic Statistics*; Brace Harcourt Jovanovich: Kent, U.K., 1985.
- Berlman, I. B. *Energy Transfer Parameters of Aromatic Compounds*; Academic Press: New York, 1973.
- Lakowicz, J. R. *Principles of Fluorescence Spectroscopy*; Plenum Press: New York, 1983.
- Berlman, I. B. *Handbook of Fluorescence Spectra of Aromatic Molecules*; Academic Press: New York, 1971.
- Birks, J. B. *Photophysics of Aromatic Molecules*; Wiley-Interscience: New York, 1970.
- The short component of the lifetime, τ_2 , varied from 6.4 to 10.1 ns for the PI-P/PI-A mixed solutions. There was no consistent trend to this variation. In all cases, the fractional intensity associated with the long lifetime, τ_1 , was at least 70% and was generally above 80%.
- Joanny, J. F.; Grant, P.; Turkevich, L. A.; Pincus, P. *J. Phys. (Paris)* **1981**, *42*, 1045.
- Kirste, R. G.; Lehnen, B. R. *Makromol. Chem.* **1976**, *177*, 1137.
- Mendelsohn, A. S.; Olvera de la Cruz, M., to be submitted for publication.
- Gradshteyn, I.; Ryzhik, I. M. In *Table of Integrals, Series, and Products*; Jeffrey, A., Ed.; Academic Press: New York, 1980.